

RENOVATION OF A BRIDGE USING GFRP REINFORCED CONCRETE SLABS (DVD PROCEEDINGS)

David Ďurech

Brno University of Technology, Faculty of Civil Engineering, Czech Republic, durech.d@fce.vutbr.cz

Petr Štěpánek

Brno University of Technology, Faculty of Civil Engineering, Czech Republic, stepanek.p@fce.vutbr.cz

David Horák

Brno University of Technology, Faculty of Civil Engineering, Czech Republic, horak.d@fce.vutbr.cz

Summary

The article deals with the reconstruction of a small pedestrian bridge, namely the bridge deck. The current structure is made of two main steel girders overlapped by thick steel plates with glued concrete pavement. The present condition of the bridge is very bad. Although the bearing capacity of the main girders is still flawless, the state of the upper slab and pavement is the very opposite. The pavement is damaged in lot of places and has often been pulled off its base. The steel plates and railings have been attacked by corrosion in many locations and rusted to a significant depth.

For the intended reconstruction, the use of thin concrete panels reinforced with GFRP bars to replace the original steel plates has been proposed. The steel railings are to be replaced with railings made of FRP materials as well. The use of high value materials allows the minimization of the needed concrete cover and thus the minimization of the panel's thickness by avoiding ballast material. Also, the use of modern materials effectively removes the need for almost any future maintenance and repair work. In this way, the slightly higher initial costs of the reconstruction will be compensated for by lower operating costs and a longer lifetime.

The report shows some aspects of the design of the reconstruction - starting with the comparison of possible materials and their advantages (both in the short and long-term views), moving through the actual design of the structure reinforced with GFRP materials and finally ending with mathematical models and experiments corresponding to them.

Keywords: GFRP reinforcement, mathematical modelling, reconstruction

1 Introduction

In order to meaningfully use the experience gained during several years of development of a FRP reinforcement system ([1] and [2]), it was planned that the research project would end with a pilot structure that could demonstrate the benefits of using non-metallic reinforcement in structural elements exposed to an aggressive environment. This project is now underway within the framework of a research project carried out by FAST VUT in collaboration with PREFA Kompozity a. s. [3] and PREFA Brno a. s.. A specific sort of pilot realisation was chosen with regard to the maximal utilization of the positive qualities of the composite materials used in real conditions. The desired requirements were fulfilled

by a pedestrian bridge over the river Hloučela in the town of Mostkovice (Prostějov district), the walkway layer of which has already become extensively degraded. The execution of this project will involve the first use of inner FRP reinforcement during reconstruction work in the Czech Republic. The following text describes the design of the precast concrete bridge deck.

2 Construction design

2.1 Current situation

The bridge is 13,5 m in length and 1,35 m in width. The main load bearing part of the structure is made of two steel beams of 450 mm in height, which carry the steel plate with an 80 mm-thick concrete surface layer. The concrete layer is now nearly in a hazardous condition due to the impacts of the weather and insufficient maintenance during its service life. Such a condition (**Fig. 1** and **Fig. 2**) requires immediate reconstruction. After the consideration of possible reconstruction alternatives it was decided to create new ascendable layer (deck) laid on the existing steel beams.



Fig. 1 Side view of the bridge – current condition



Fig. 2 View of the upper walkway layer – current condition

2.2 Advantages of using composite reinforcement

The pilot structure was designed in the form of precast concrete panels reinforced by non-metallic composite reinforcement based on glass fibres in epoxy matrix. Such composite reinforcement (whether glass, carbon or aramid-based) has several advantages in comparison with standard steel reinforcement. Generally these types have:

- high resistibility against corrosion,
- high resistibility against chemical effects,

- no voltaic conductivity,
- no magnetism,
- low heat conductivity,
- low volume weight.

In this case, the decisive aspect was mainly the resistibility against environmental influences, which allows minimisation of the concrete cover. The thickness of the concrete cover is determined only by the adhesion between the reinforcement bars and concrete to ensure sufficient anchoring of the bars. In combination with the low volume weight it is even possible to increase the sizes of new parts of the construction without increasing the load on the bearing structure (comparison in **Fig. 3** and **Tab. 1**). Thanks to this, the pavement width will be extended so that two-way pedestrian traffic will be easier, which was one of the main requirements for the new construction.

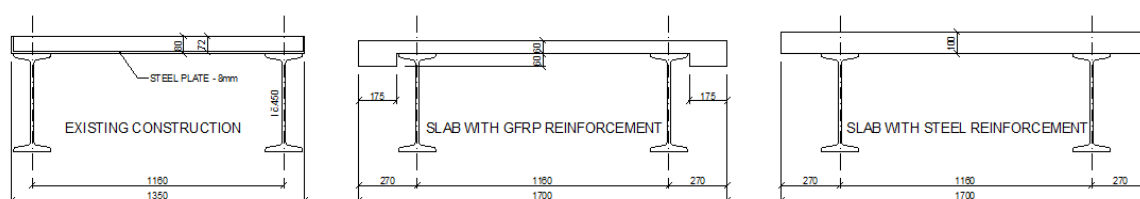


Fig. 3 Solution variants

Tab. 1 Dead load comparison of design solutions per 1m'

	[kN]	[%]
Existing construction	3,203	100
Slab with GFRP reinforcement	2,829	88,3
Slab with steel reinforcement	4,25	132,7

The weights used for the calculation in Table 1 are 23 kN/m³ for plain concrete, 22 kN/m³ for GFRP reinforcement and 78,6 kN/m³ for steel.

2.3 Panel design

The design and calculation were prepared according to ACI 440.1R-03 [5] standards intended for concrete structures reinforced by FRP reinforcement. Individual forms of load cases and their combinations were determined according to Czech Republic standards [6] [7] [8] [9]. Because the bearing capacity calculation was carried out for the concrete panel according to the ACI standard, the partial safety coefficients had to be harmonized to maintain the desired overall safety level of the resulting design.

2.3.1 Loads

There were several forms of load cases considered during the design phase:

- the self-weight of the construction,
- wind load,
- the uniform effective load (across the whole width of the panel, i.e. also on the cantilevered ends),
- isolated loads (which exclude the uniform load in the load combinations),
- assembly loads during transportation of the panel.

Because the panels are designed to be directly ascendable, the dead load consists only of the self-weight of the concrete panel and the weight of the railings. The wind load was decisive for the stability check together with the slight dimensions of the designed panels, which result in the low weight of the final structure. In this specific area, the snow load is quite low (significantly lower than effective loads caused by pedestrians). Considering that and the fact that the bridge is meant only for pedestrians, the snow load wasn't included in combination with the full effective load. The influence of changing temperature is taken into consideration in the design of the necessary reinforcement area. Extreme loads, caused by a utility car driving onto the bridge, are not possible because of the small width of the bridge. Only the load forces caused by a small utility vehicle were checked.

2.3.2 Bearing capacity - bending

The real physical mechanical properties of the GFRP reinforcement were determined during performed tensile strength tests and were defined by the average tensile strength, its standard deviation and modulus of elasticity.

The guaranteed tensile strength was determined according to [5]. To define the design value it is necessary to lower the measured tensile strength by a reduction multiplier that takes account of environmental influences. Its value, $C_E = 0,7$ is given for concrete structures and non-metallic reinforcement freely exposed to environmental influences. The modulus of elasticity is calculated from its average value measured during the tests. The next step is to determine the limit strain of the reinforcement and the balanced reinforcement ratio.

Average tensile strength (1), standard deviation (2):

$$f_{u,ave} ; \sigma \quad (1), (2)$$

Guaranteed tensile strength (3):

$$f_{fu}^* = f_{u,ave} - 3 \cdot \sigma \quad (3)$$

Design tensile strength (4):

$$f_{fu} = C_E \cdot f_{fu}^* \quad (4)$$

Modulus of elasticity (5):

$$E_f = E_{f,ave} \quad (5)$$

Limit strain (6):

$$\varepsilon_{fu} = \frac{f_{fu}}{E_f} \quad (6)$$

Balanced reinforcement ratio (7)

$$\rho_{fb} = 0,85 \cdot \beta_1 \cdot \frac{f_c'}{f_{fu}} \cdot \frac{E_f \cdot \varepsilon_{cu}}{E_f \cdot \varepsilon_{cu} + f_{fu}} \quad (7)$$

In the reinforcement ratio formula the limit strain for concrete is given by the value $\varepsilon_{cu} = 0,003$ (according to the ACI standard); f_c' is specified as the concrete's compressive

strength; β_1 is a coefficient modifying the concrete's compressive strength (it depends on the compressive strength of the concrete).

The balanced reinforcement ratio then determines the failure mode of the structure. If $\rho_f > \rho_{fb}$ then the structure will collapse during the reinforcement rupture; if $\rho_f < \rho_{fb}$ then the structure will collapse during concrete crushing. The panels are designed so that the limit state is caused by the latter (**Fig. 4**).

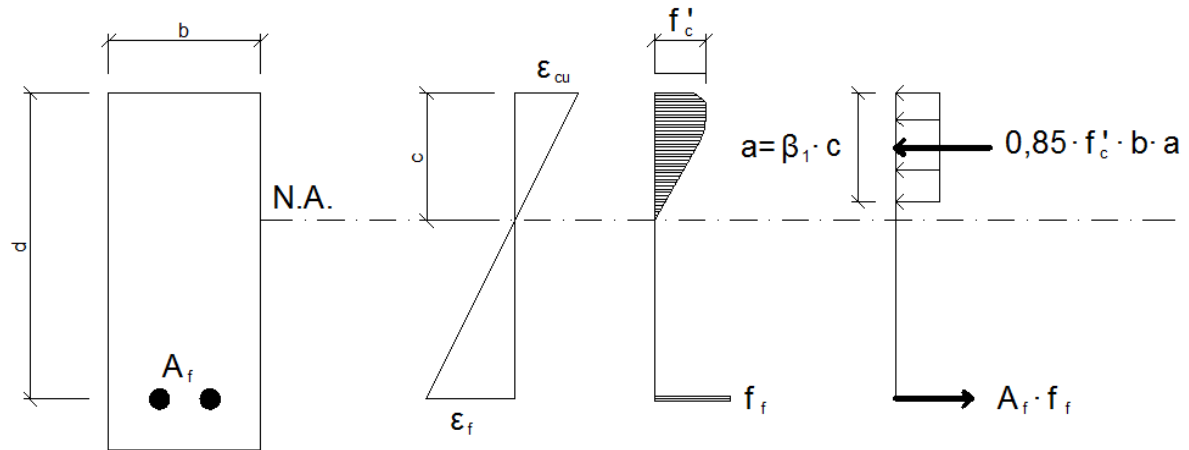


Fig. 4 Ultimate limit state - concrete crushing

Before calculating the bearing capacity, the stress in the reinforcement and the nominal moment capacity of the member have to be determined. If the prerequisite $\rho_f > 1,4\rho_{fb}$ is satisfied then the following applies:

Stress in the reinforcement (8):

$$f_f = \left(\sqrt{\frac{(E_f \cdot \varepsilon_{cu})^2}{4} + \frac{0,85 \cdot \beta_1 \cdot f'_c}{\rho_f} \cdot E_f \cdot \varepsilon_{cu}} - 0,5 \cdot E_f \cdot \varepsilon_{cu} \right) \leq f_{fu} \quad (8)$$

Nominal bending moment capacity (9):

$$M_n = \rho_f \cdot f_f \cdot \left(1 - 0,59 \frac{\rho_f \cdot f_f}{f'_c} \right) \cdot b \cdot d^2 \quad (9)$$

Reliability condition (10):

$$\phi \cdot M_n \geq M_u \quad (10)$$

where $\phi = 0.7$ and M_u is the maximal moment from all load combinations.

2.3.3 Bearing capacity – shear

To correctly determine the shear capacity of the cross-section it is necessary to take into account the following differences between steel and FRP reinforcement:

- FRP materials have a lower modulus of elasticity than standard steel reinforcement (depending on the material and fibre ratio in the FRP reinforcement bar).

- FRP reinforcement has high tensile strength but it lacks the plastic part in the stress-strain diagram.
- Reinforcement formed by bending has lower tensile strength than straight reinforcement bars.
- FRP reinforcement has low shear strength.

In our case the panel is designed to be without shear reinforcement. Therefore, all the shear resistance is generated only by the concrete. When comparing a FRP reinforced member and a classical steel reinforced member it is possible to obtain the relation needed for defining the shear bearing capacity (11):

$$V_{c,f} = \frac{\rho_f \cdot E_f}{90 \cdot \beta_1 \cdot f_c'} \cdot V_c \leq V_c; \text{ where } V_c = \frac{\sqrt{f_c'}}{6} \cdot b \cdot d \quad (11)$$

2.3.4 Serviceability

Concrete structures reinforced with non-prestressed FRP reinforcement (with a relatively low modulus of elasticity) are expected to suffer from bigger crack widths in comparison to steel reinforced concrete. For most cases, standard [5] recommends using the limitations quoted by the Canadian Standards Association (1996). In these recommendations the maximum allowed crack width is $w = 0,5$ mm for structures exposed to an outdoor environment and $w = 0,7$ mm for structures placed inside buildings. The exceptions are structures placed in an aggressive environment, or watertight structures. If a structure suffers from crack propagation then the maximum crack width can be determined using the relation (12):

$$w = \frac{2.2}{E_f} \cdot \beta \cdot k_b \cdot f_f \cdot \sqrt[3]{d_c \cdot A} \quad (12)$$

where β is the ratio given by the distance between the neutral axis and the pulled edge of the cross section, and by the distance between the neutral axis and the centre of gravity of the pulled reinforcement; d_c is the distance between the centre of gravity of the pulled reinforcement and the pulled edge of the cross section; A is the cross-section area; k_b is the rate of adhesion between the reinforcement and the concrete (for steel reinforcement and steel-like FRP reinforcement this rate is $k_b = 1,0$; for FRP reinforcement with higher adhesion $k_b < 1,0$ should be used, for the FRP reinforcement with lower adhesion an adequate value of $k_b > 1,0$ should be used; if the adhesion between the reinforcement and the concrete is not known, the recommended value is $k_b = 1,2$).

There are two possible methods of checking the deflection of the structure. The first is based on the bending stiffness control, where reaching a sufficient value of stiffness guarantees the resulting deflection within the given limits. Although usable for steel reinforced concrete members, this method is not suitable for FRP reinforced members and can be used as the preliminary design method only. The second method uses direct calculation of the deflection. To solve the relation it is necessary to evaluate the bending stiffness $E_c I$ of the member. The value ranges from the stiffness value $E_c I_g$ (the cross-section at the beginning of crack propagation) to the value $E_c I_{cr}$ (the cross-section with a fully developed crack). To determine the moment of inertia of the member the following relation can be used, while taking the linear behaviour of the FRP reinforcement into account (12):

$$I_e = \left(\frac{M_{cr}}{M_a}\right)^3 \cdot \beta_d \cdot I_g + \left[1 - \left(\frac{M_{cr}}{M_a}\right)^3\right] \cdot I_{cr} \leq I_g \quad (12)$$

where the coefficient covering the behaviour of the FRP reinforcement is given by (13):

$$\beta_d = \alpha_b \cdot \left[\frac{E_f}{E_s} + 1\right] \quad (13)$$

the coefficient $\alpha_b = 0,5$ is the same for all types of FRP reinforcement.

The further process of calculating the bending stiffness of the member is the same as for the steel reinforced concrete members.

2.3.5 Creep and fatigue

To avoid dangerous phenomena caused by creep or fatigue (i.e. brittle fracture) it is necessary to limit the tension in the reinforcement. The calculation of the current tension in the bars is identical for the creep check and for the fatigue check. It is based on the elastic behaviour of the reinforced cross-section (**Fig. 5**) and can be calculated using the relation (14):

$$f_{f,s} = M_s \cdot \frac{n_f \cdot d \cdot (1-k)}{I_{cr}} \quad (14)$$

If a creep check is performed, the value M_s is evaluated from the load combination containing the dead loads and the long term acting service loads. If a fatigue check is desired, the value M_s has to be increased by the bending moment induced by the fatigue load cycle. Both cases have to fulfil the reliability condition defined as (15) (for GFRP reinforcement):

$$f_{f,s} \leq 0.2 \cdot f_{fu} \quad (16)$$

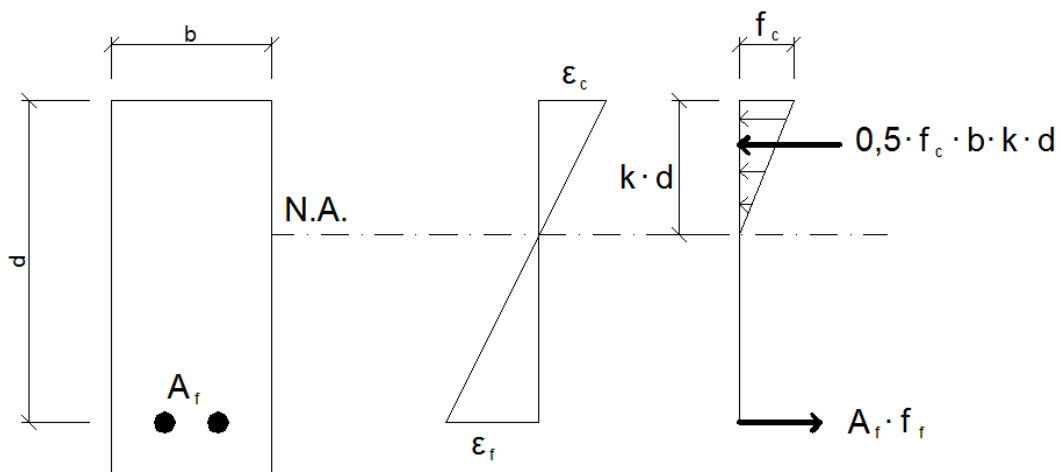


Fig. 5 Inner forces along the cross-section used for fatigue and creep checks

2.3.6 Final design

During the reconstruction the bridge deck will be replaced together with the railings. The new bridge deck is designed in the form of precast concrete panels with a length of 1,5 m,

reinforced with GFRP reinforcement. The placement of the reinforcement is shown in **Fig. 6**. The ascendable surface of the panels is designed to be without any additional protective layer. The existing corroded railings are to be replaced by composite railings. They will be anchored to the concrete panels using a non-metallic anchoring system. The use of composite materials should eliminate the need for maintenance work on the railings.

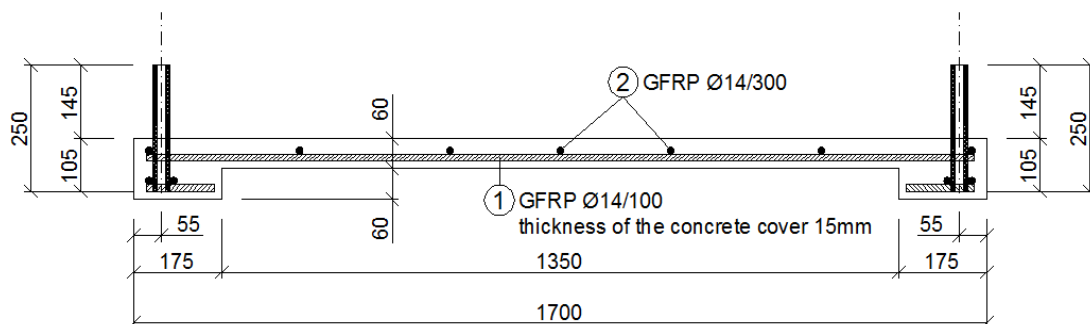


Fig. 6 Reinforcement of the panel

3 Verification experiments

3.1 Numerical model

All experiments were prepared as numerical simulations first. The models were prepared in ATENA FEM software [4]. The applied boundary conditions were defined in such a way that they characterize the situation during real testing and their real use as accurately as possible. A scheme of the experiment is shown in **Fig. 7**.

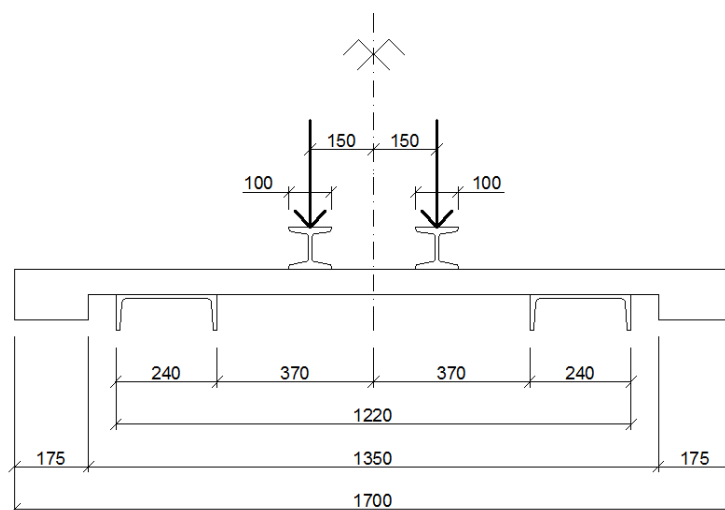


Fig. 7 Scheme of the experiment

Given the symmetric geometry of the panel and also the loading scheme, the model was prepared as axially symmetrical. As only one half of the panel was calculated, it was possible to use a more detailed model without difficulties arising from the presence of too many FE. The panel was modelled as a 2D and also a 3D simulation. Thanks to the

relatively simple shape of the panel, the 2D model provided very accurate results and therefore the 3D simulation was used for reference calculations only.

The concrete's material characteristics were assigned according to the results of real experiments performed on separate material samples (see **Table 2**). The individual variables were drawn from the experiment results in their mean values.

Tab. 2 Material characteristics used in the numerical model for concrete

Concrete	
Tensile bending strength [MPa] – experimentally measured	5,892
Crushing strength [MPa] – experimentally measured	50,872
Modulus of elasticity [MPa] – experimentally measured	32800
Fracture energy [MJ/m ²] – default value	8e-5
Density [MN/m ³]	0,023

The spread footing under the load force was modelled as a plain elastic material with material characteristics corresponding with standard steel (i.e. modulus of elasticity $E = 200$ GPa, Poissons ratio 0,3).

The real physical mechanical properties of GFRP reinforcement were determined during tensile strength tests performed as a part of the development of the reinforcement [2]. The non-metallic reinforcement behaves as a linear elastic material until sudden rupture occurs. The same stress-strain dependency was modelled in the numerical material model. The elastic branch of this diagram (Fig. 8) is inclined in accordance with the measured modulus of elasticity, $E_{f,ave} = 35\ 693$ MPa.

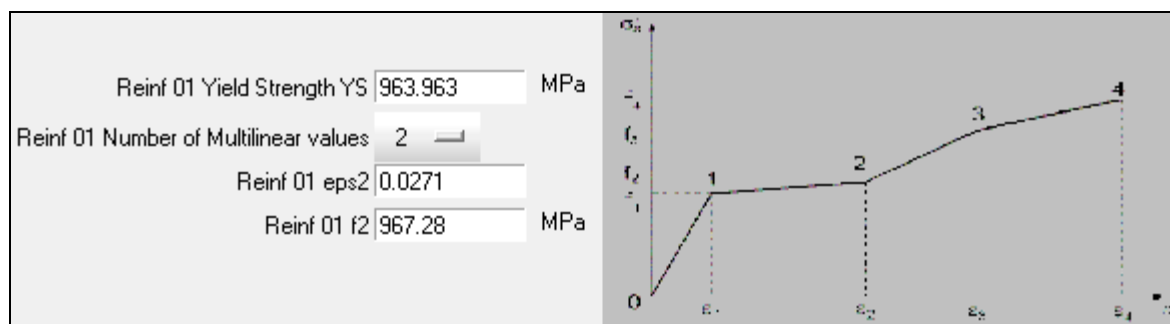


Fig. 8 Stress-strain diagram of the GFRP reinforcement

The loading of the panel is defined by the deflection of the spread footing (i.e. the model is loaded by the deformation). The supports are defined in the edge points of the supporting beams. This simulates the rotation of a panel around a stiff support as was observed and confirmed in the real experiment. Such boundary conditions also allow the observation of the behaviour of the concrete in the area near the support, and the controlling of the risk that the concrete will be crushed. The symmetry of the model was achieved by applying adequate supports in the axis of symmetry of the panel.

To obtain data comparable with the real experiment, the deflection of the panel, the acting/resisting forces and the tension in the reinforcement were monitored. Exact measuring points are shown in **Fig. 9**; these points correspond with those in the real experiments.

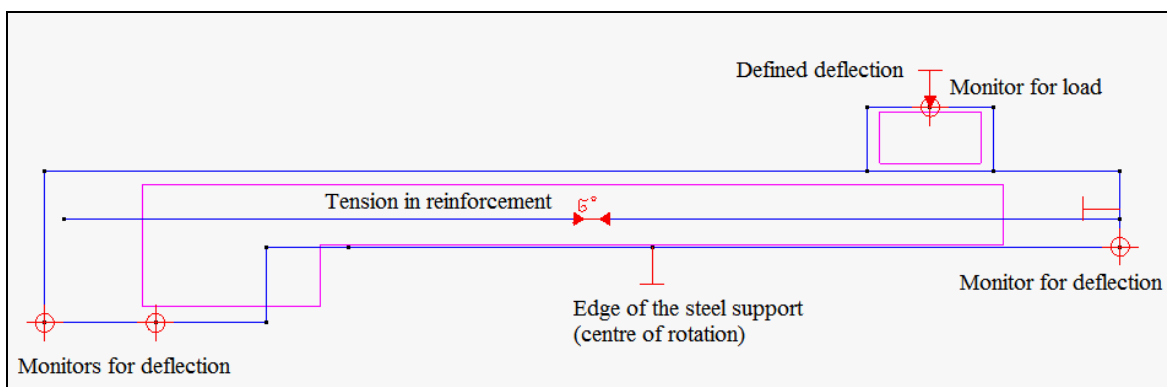


Fig. 9 Detail of the boundary conditions in the numerical model

After the calculation, all of the important values which characterize the ultimate limit state of the designed panel were obtained:

- maximal load force is 59,3 kN,
- maximal tensile stress in the reinforcement is 275 MPa,
- the failure of the panel is caused by crushing of the concrete (i.e. reaching the compression strength of the concrete),
- maximal deflection in the middle of the span is 13,8 mm; the non-loaded panel edge was raised by 24,6 mm (see **Fig. 10**).

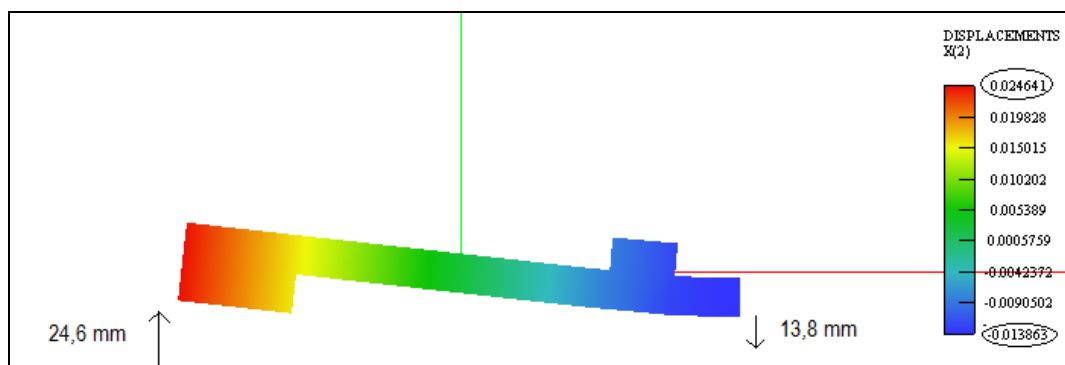


Fig. 10 Deflection of the specimen

3.2 Experimental verification

The values and the behaviour of the panel obtained from the numerical model were verified by real experiments. All supports and loading were set up according to the future use of the panel and the numerical model. The setup scheme of the real load test is shown in **Fig. 11**.

The test specimen failed as the concrete was crushed (see **Fig. 12**) in the middle of the panel, as was predicted in the numerical and design model. During the experiment all the data stated in the description of the numerical model were collected and afterwards compared with the theoretical results (**Fig. 13** and **Table 3**).



Fig. 11 Testing of the panel



Fig. 12 Collapsed specimen (crushed concrete has been removed)

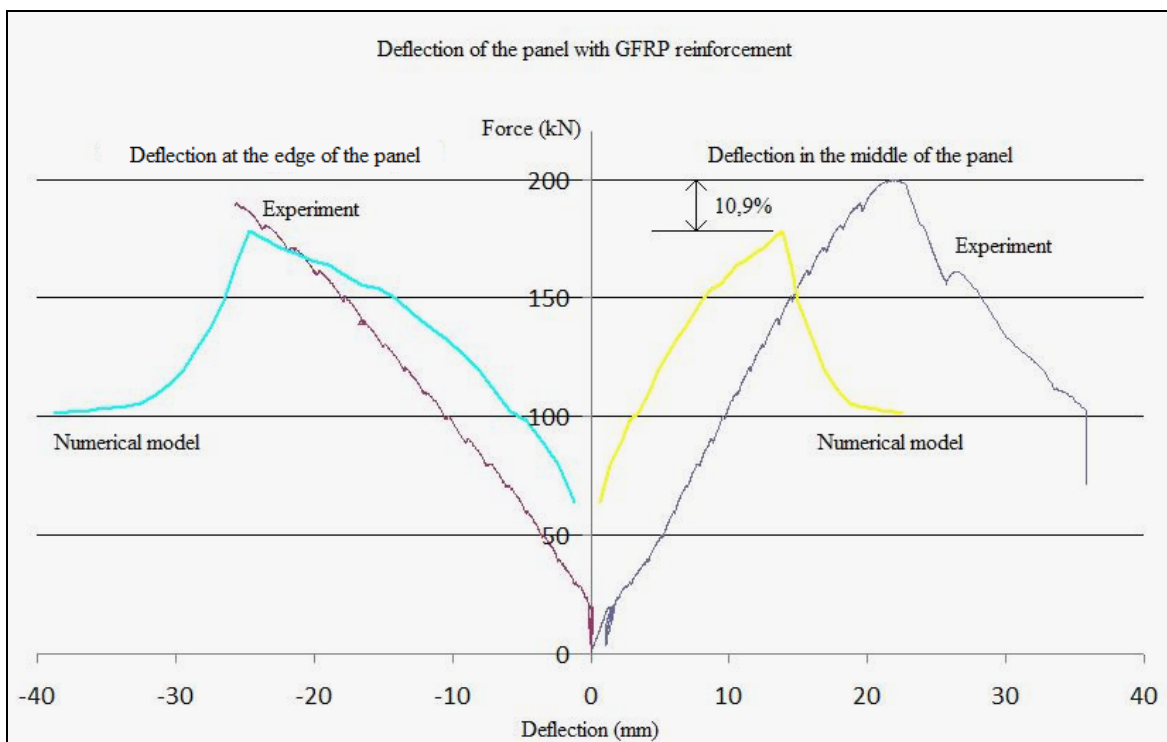


Fig. 13 Comparison of the numerical model and the real experiment

Tab. 3 Comparison of the numerical model and the real experiment

Numerical model	Experiment	Difference
$F_{max}=177,9\text{kN}$	$F_{max}=199,7\text{kN}$	10,9%
$u_{max}=13,8\text{mm}$	$u_{max}=18\text{mm}$	23%
$M_{max}=15,1\text{kNm}$	$M_{max}=16,9\text{kNm}$	10,6%

In **Fig. 14** the value of the total force is gained from the sum of all load forces acting on the test specimen. The comparison in **Table 3** shows a relatively good match between the numerical model and the real experiment. The deflection of the panel is re-calculated as the average value along the length of the panel.

The conclusion based on the comparison of the results confirms the ability of the designed panels to resist loading and thus the possibility of their use for the intended reconstruction. The practical verification of the bearing capacity and the overall behaviour of the panel were especially important because new materials are being used whose use is not yet covered by national standards.

4 Conclusion

During this reconstruction only a few of the advantages of FRP reinforcement are used, but despite that, the final structure profits from it. The higher cost of the reinforcement is compensated for by the material savings because the necessary concrete cover is only minimal, and due also to the high tensile force of the reinforcement the concrete panel can be designed as a very slender construction. Other savings are gained by the elimination of any additional protective preparations - the concrete and the reinforcement itself are capable of withstanding the impacts of the environment. Also, the railings made of composite materials need no additional coating or any special service. By using modern materials the future maintenance of the structure should be limited to regular inspections only.

The final structure will be additionally equipped with measuring points, which allow the monitoring of the behaviour and the state of the structure over time. The gained results will be used for further study and evaluation of the long term behaviour of composite structures.

This sample structure shows that the use of composite reinforcement offers an interesting and competitive alternative to steel reinforcement, especially when including the usability, protection and maintenance work savings.

The presented results were obtained with the financial support of the Czech Science Foundation within the framework of project 103/09/H085 - "Modern composite structures" and project FR-TII/357 – "Concrete structures with non-metallic reinforcement with increased heat and aggressive environment resistibility" supported by the Czech Ministry of Industry and Trade. Some results were obtained from project 1M0579 – CIDEAS (financially supported by the Ministry of Education, Youth and Sport).

References

- [1] Pavel Krůpa, David Horák, Petr Štěpánek. *Vláknové kompozity jako hlavní výztuž betonu*. Contribution to the VUSTAH 2007 conference in Telč
- [2] Pavel Krůpa, David Horák, Jan Fojtl, Petr Štěpánek. *Fyzikálně-mechanické vlastnosti nekovových výztuží ze skelných a uhlíkových vláken a jejich soudržnost s betonem*. Contribution to the Betonářské dny conference in Bratislava, 2006
- [3] <http://www.prefa-kompozity.cz>
- [4] Procházková Zdenka, Červenka Jan, Janda Zdeněk, Pryl Dobromil. *Atena science – GID Tutorial*. Prague, 2009
- [5] ACI 440.1R-03 Guide for the Design and Construction of Concrete Reinforced with FRP Bars

- [6] ČSN EN 1991-1-1 Zatížení konstrukcí, Obecná zatížení – Objemové tíhy, vlastní tíha a užitná zatížení pozemních staveb
- [7] ČSN EN 1991-1-3 Zatížení konstrukcí, Obecná zatížení – Zatížení sněhem
- [8] ČSN EN 1991-1-4 Zatížení konstrukcí, Obecná zatížení – Zatížení větrem
- [9] ČSN EN 1991-2 Zatížení konstrukcí – Zatížení mostů dopravou